

# The Effect of Printing Parameters on Scaffold Structure Using Low-cost 3D Printer

Nor Aiman Sukindar<sup>1,\*</sup>, Azib Azhari Awang Dahan<sup>1,b</sup>, Nor Farah Huda Abd Halim<sup>1,c</sup>, Shafie Kamaruddin<sup>1,d</sup>, Mohd Hafis Sulaiman<sup>1,e</sup>, Mohd Khairul Anuar Mohd Ariffin<sup>2,f</sup>

<sup>1</sup>Department of Manufacturing and Materials Engineering Kulliyyah of Engineering International Islamic University Malaysia 53100, Gombak, Selangor Malaysia

<sup>2</sup>Department of Mechanical and Manufacturing, Universiti Putra Malaysia, 43400 Serdang, Selangor, Malaysia

## Article Info

Volume 82

Page Number: 8255 - 8263

Publication Issue:

January-February 2020

## Abstract:

Additive Manufacturing (AM) technologies had widely used in most of the application such as aeronautics and automotive industries, for tooling and casting parts and even for medical purpose. These wide applications can be achieved by utilizing AM in the daily manufacturing process due to its capabilities to manufacture parts with complex shapes with no significant material removal process. In medical applications, the 3D printing method was used to fabricate bone support structure or known as scaffold structure. The ability of this technology in the fabrication of the scaffold structure lies by manipulating printing parameters to achieve desired porosity. This research investigated the effect of different porosity levels on a scaffold structure in terms of Equivalent Von-Mises Strain and Total Deformation. The porosity level was created by varying printing parameters including layer height, infill density, and shell thickness by slicing the initial solid CAD file using Repetier Host 3D printing software. The research mainly based on the Finite Element Analysis (FEA) in which the created scaffold structures were simulated to check its capability when different porosity on the design was applied. The simulation result indicates that the increase of porosity level will result in higher total deformation of the structure. Therefore, by manipulating the printing parameters, different levels of porosity structures can be achieved.

## Article History

Article Received: 18 May 2019

Revised: 14 July 2019

Accepted: 22 December 2019

Publication: 07 February 2020

**Keywords:** Open-source 3D printer, Printing parameters, FEA analysis, Scaffold design.

## 1. INTRODUCTION

Earlier studies had recognized numerous benefits for the manufacturing industry from Additive Manufacturing (AM) manufacturing process. Referring to the American Society for Testing and Materials (ASTM) F42 Technical Committee, they had defined that Additive Manufacturing (AM) as the process of joining materials to produce items from 3D model information, generally layer by layer, as opposed to subtractive production methods[1]. Furthermore, the technology had been extensively studied for research and business and it has demonstrated an excellent capacity to produce parts for a variety of apps,

eliminating various production limitations and generating architecture with more complex geometry than standard techniques[2].

Fused Deposition Modelling (FDM) working principles had been discussed by Chen where firstly the extruder in FDM executes the extrusion of semi-molten materials in filament and deposits them layer by layer onto the printing platform[3]. Other research shows that the material in the filament is melted into a specially designed head that extracts a surface from a prepared 3D CAD template according to the segment data generated[4]. As it is extruded, the template is cooled and therefore solidified. As with other RP techniques, the design is constructed by

stacking and depositing each layer successively from the bottom to the top.

The flexibility of FDM process makes this technology has been widely used in many applications including the medical field. As researched by Too et al. , they used FDM1650 to create 3D non-random porous structures (scaffolds) in ABS and tested the structures to test their TE functionality [5]. Researchers also studied the impact of FDM system parameters on porosity, pore depth, and porous structures compressive strength. Other research by Jyoti et al. employed FDM system to create and assemble polymer-ceramic composite scaffolds containing polypropylene polymer and tricalcium ceramic phosphate of various porosities utilizing specific FDM parameters and design types[6]. They performed mechanical tests and in vitro cell experiments on the scaffolds and found that during the first 2 weeks of in vitro research the cells were non-toxic with excellent cell growth. Next, Owida and Chen had using hybrid FDM and coronary artery bypass graft (CABG) electrospinning techniques[7]. For the manufacture of the engineered artery graft, they used FDM3000 to make an exact CABG mold made of ABS for use as the electrospinning surface collector and then used electrospinning and rotary selection methods to create nanofibrous tubular scaffolds with optimal design.

The recent study also focusing on medical porous scaffold regarding its application and potential. In 2018, the elements used to formulate novel pore PLGA / TCP / Mg (PTM) scaffolds using low-temperature rapid-prototyping (LT-RP) technology include magnesium (Mg) poly, lactide (co-glycolide) (PLGA),  $\beta$ -tricalcium phosphate ( $\beta$ -TCP)[8]. The study had found that the PTM scaffold has a well built and mechanically enhanced bio-mimic structure. Dynamic contrast-enhanced magnetic resonance imaging (DCE-MRI) and microcomputing (MCC) angiography showed that PTM scaffold could increase infusion into the blood and encourage new vessel growth four weeks after surgery. In comparison, many newly formed vessels with a sound architectural structure were observed at 8 weeks after surgery. Besides, research on porous titanium alloy scaffolds for bone tissue repair also had been studied [9]. By using modeling parameterization, novel porous structures were developed. The exact models of key features,

including porosity and the mechanical character of scaffolds, have been studied and the outcome exhibits that the parametric modeling of porous titanium bone tissue engineering fabrics with good mechanical and biological properties have been achieved through the design, manufacturing, characterization and evaluation of porous scaffold structures. In addition, the medical application continue with fabrication of porous Mg-Zn scaffold where a highly pored magnesium-zinc (Mg-Zn 4 wt.%) and a variety of ethanol concentrations (0 vol. % to 40 vol. %) were provided by the adjusted replica process, with a different rates of liquid media (50 wt. % to 90 wt. %)[10]. Therefore, the results of X-ray diffractometer (XRD) and of the compression test show that ethanol consumed by the liquid replica media results in 46 percent higher level stress due to a lower Mg-water response and no scaffold formation of  $\text{Mg}(\text{OH})_2$ . The findings of porosity measurements show that the composition of the mixture of water-ethanol and various solid fractions have no significant effect on the actual apparent porosity of the manufactured scaffolds.

The primary problem in biomedical implementation for applying Additive Manufacturing (AM) is the higher cost of the AM machine. Higher machine costs will result in greater medical service costs. Emphasized by Tan et al., they stated that in medical applications, patient-specific cranioplasty implants that are commercially accessible are anatomically precise but expensive[11]. Besides, as researched by Kahl et al., they emphasized that due to its tremendous potential beyond its typical applications, 3D bio-printing has become a versatile and strong technique in tissue engineering and regenerative medicine[12]. However, 3D bioprinting technologies that are commercially accessible are typically costly to overcome wide applications. The present study focuses on manipulating the process parameters to achieve different porosity levels by using a low-cost 3D printer. FEA analysis has been used to examine the different printing parameters which will result in different porosity levels.

**2. METHODOLOGY**

In this research, FEA analysis has been used to investigate the capability of low-cost 3D printer in fabricating the scaffold structure. The Equivalent Von Misses Strain and Total Deformation were observed to see the effect of porosity level using different printing parameters.

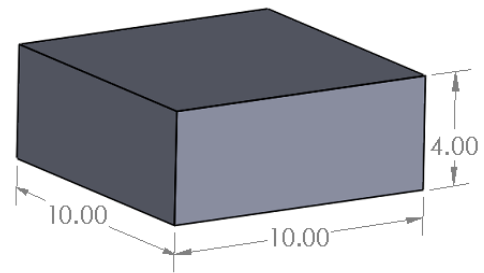


Figure 1: Design sample for the simulation

**2.1 Design Sample**

In this research, polymethylmethacrylate (PMMA) material was used with the thermal conductivity of 0.19 W/m·K. The melting point of the PMMA is 220°C, the specific heat is 1,600J/kg·K, and the density is 1.18 g/cm<sup>3</sup>. The scaffold was designed by using Solidworks (Dassault Systèmes, MA) with a dimension of (10 x 10 x 4) mm according to ISO 604 from previous research. The solid design sample and its dimensions were shown in Figure 1.

**2.2 Design of Experiment**

Among several parameters affecting the mechanical properties of 3D-printed porous scaffold samples, three of them were chosen to be investigated in this study. The printing configuration variables are Layer Height (mm), Shell Thickness (mm), and Infill Density (mm). Design of Experiment (DOE) has been executed using Minitab 19 (Minitab, USA) software. By applying Taguchi’s method, a Taguchi orthogonal array of 3<sup>3</sup> was performed. Thus, a sum of nine samples was designed and simulated using Ansys Workbench (ANSYS Inc., USA). Table 1 shows the parameters used to perform this simulation work.

Table 1: Design of Experiment for the simulation

No	Shell Thickness, mm	Layer Height, mm	Infill Density, %
1	0.4	0.1	25
2	0.4	0.15	50
3	0.4	0.2	75
4	0.8	0.1	50
5	0.8	0.15	75
6	0.8	0.2	25
7	1.2	0.1	75
8	1.2	0.15	25
9	1.2	0.2	50

**2.2.3D-Printing Software**

The three printing parameters were chosen for the simulation and shown in Table 2. By manipulating these parameters, a variety of scaffolds with different porosity levels had been developed. Meanwhile, Figure 2 shows the design samples were converted into STL format by using Repetier-Host Software (Hot-World GmbH & Co. KG, Germany).

Table 2: Printing Parameters

Parameters	Descriptions		
Layer Height (mm)	0.1	0.15	0.2
Shell Thickness (mm)	0.4	0.8	1.2
Infill Density (%)	25	50	75

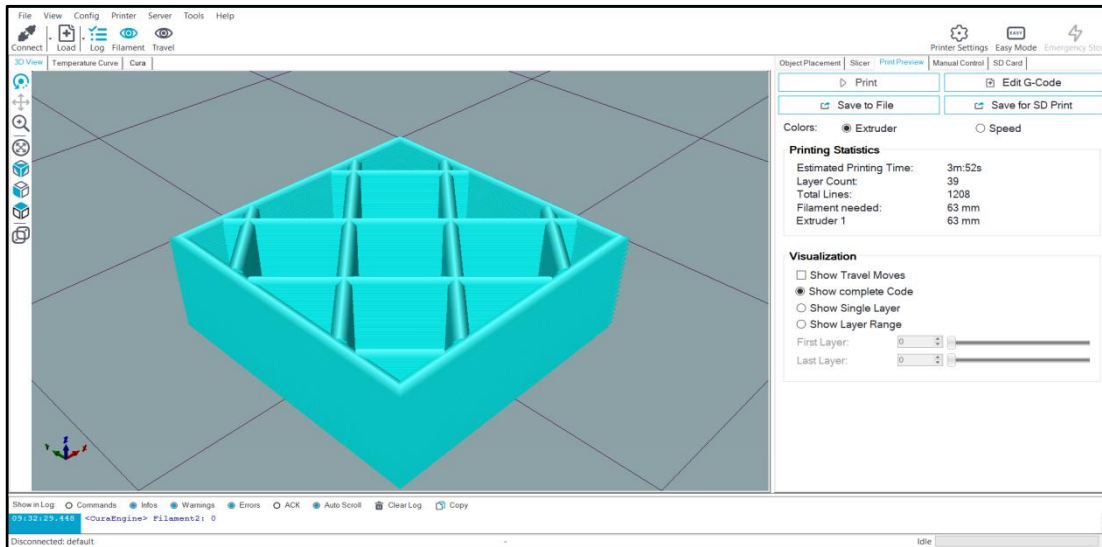


Figure 2: Sliced CAD model using the printing parameters

### 2.3 Simulation

For the simulation purposes, the analysis was carried out using Ansys Workbench 19.2 (ANSYS Inc., USA). The analysis was based on a “Static Structural” test, using a 500N load compressing the specimen based on the previous study[13]. In this research, the work was done based solely on simulation. Material properties of PMMA such as material density was used using data collected from previous experimental works. The simulation procedure starts with designing the samples with nine different parts according to the sliced solid sample shown by 3D-printer software with nine different printing configurations. All the parts were

converted into Initial Graphics Exchange Specification (IGES) format before imported into Ansys Workbench as shown in Figure 2(a). Meanwhile, Figure 3 shows the top view of the re-design samples in the CAD software. Input properties based on PMMA material properties such as density, information on elastic-plastic behaviour and yield strength were applied to the design. For the meshing process, an automatic program-controlled setting which includes physics preference, element order, mesh transition, and span angle centre were setup. The meshing process was shown in Figure 2(b). Based on the simulation, the result will be analysed in terms of Equivalent Von-Misses Strain and Total Deformation.

(a)

(b)

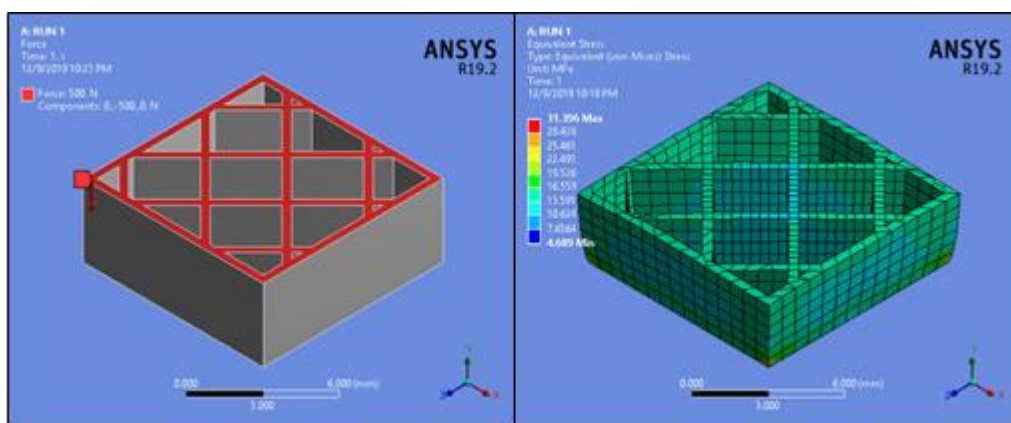
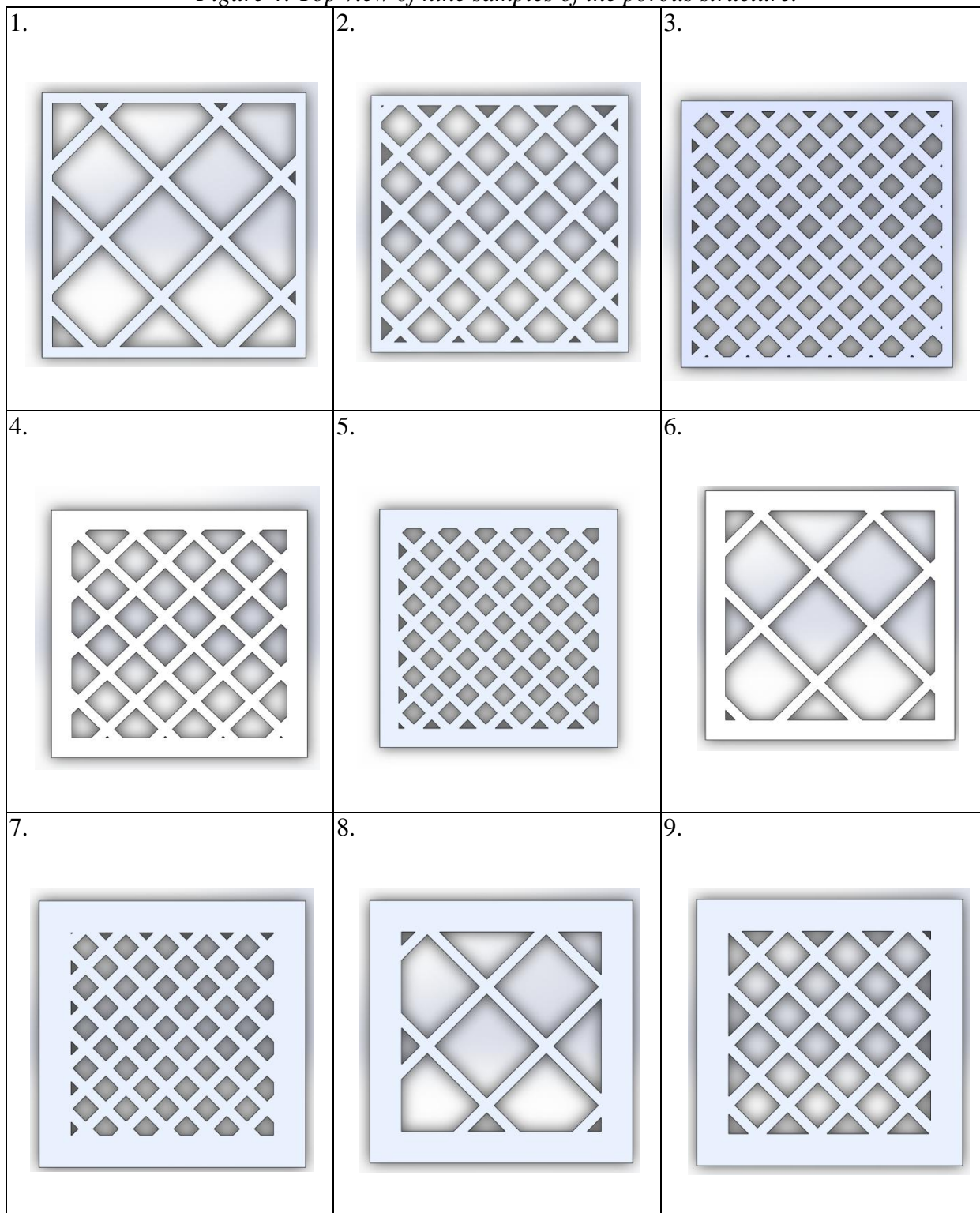


Figure 2: (a) Part converted Initial Graphics Exchange Specification (IGES) format (b) Meshing process of the sample

Figure 4: Top view of nine samples of the porous structure.



## 2.4 Porosity

The porosity of the parts was estimated using Equation 1 and 2 based on the previous study[14].

$$V_p = V_T - V_s, \text{ where } V_s = \frac{m_s}{\rho_s} \quad (1)$$

$$\text{Porosity (\%)} = \frac{V_p}{V_T} \times 100 \quad (2)$$

where  $V_p$  is the total volume occupied by the pores and  $V_T$  is the total volume of the solid scaffold which is  $400 \text{ mm}^3$ . On the other hand, the volume of  $V_p$

obtained using Equation 1 where  $V_S$  is the scaffold volume that can be accessed using Mass Properties provided in SolidWorks software.

**3. RESULTS AND DISCUSSION**

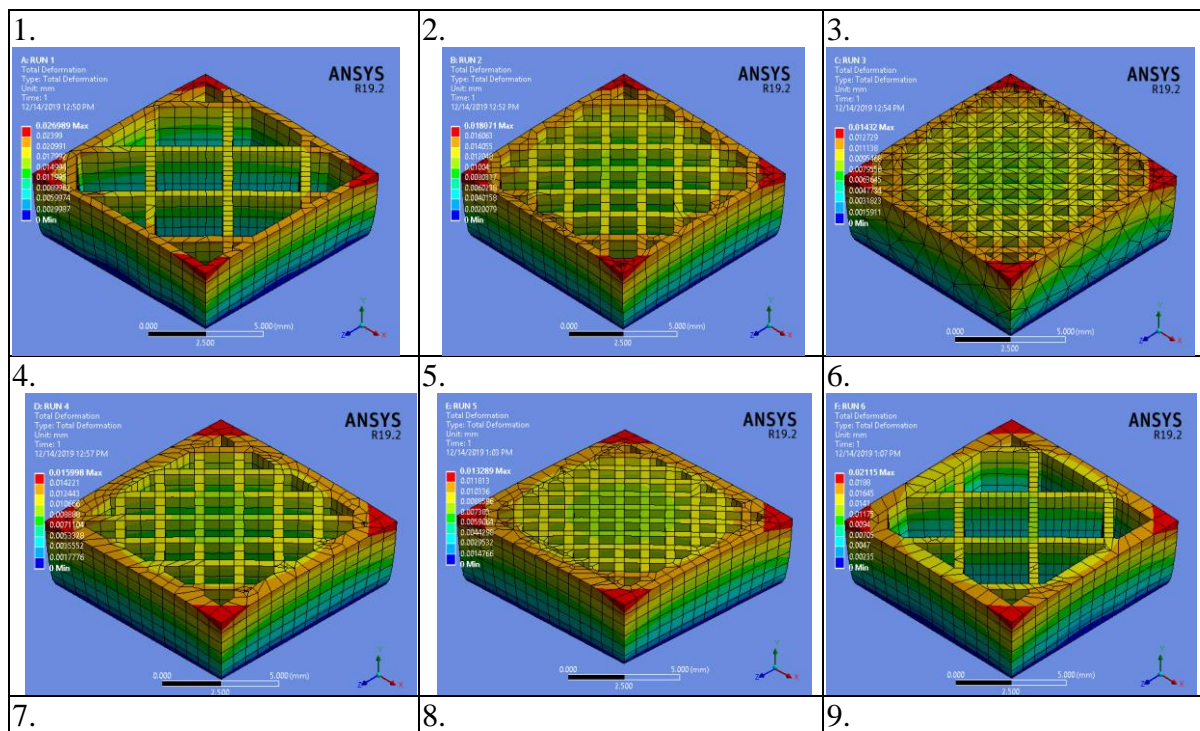
The porosity for nine sample parts was calculated by using Equation 1 and 2 as shown in Table 3. These porosity differences came from different printing parameters and these nine samples indicating the design according to DOE.

Table 3: Calculated porosity level

Number of RUN	Volume, mm <sup>3</sup>			Porosity Level (%)
	$V_T$	$V_S$	$V_P$	
1	400	140.94	259.06	64.77
2	400	210.17	189.83	47.46
3	400	268.31	131.69	32.92
4	400	239.07	160.93	40.23
5	400	288.99	111.01	27.75
6	400	183.11	216.89	54.22
7	400	309.54	90.46	22.62
8	400	222.52	177.48	44.37
9	400	271.70	128.3	32.08

Based on Table 3, it shows that different level of porosity can be achieved by manipulating the printing parameters. The low infill density, lower layer height, and shell thickness contribute to the highest porosity level. Measuring the porosity level is very crucial especially in fabricating scaffold

structure for biomedical. Meanwhile, for the simulation process, each porous structure was examined using the Static Structural Simulation using Ansys Workbench (Ansys Inc., USA). Figure 5 representing each structure after the simulation work has been carried out.



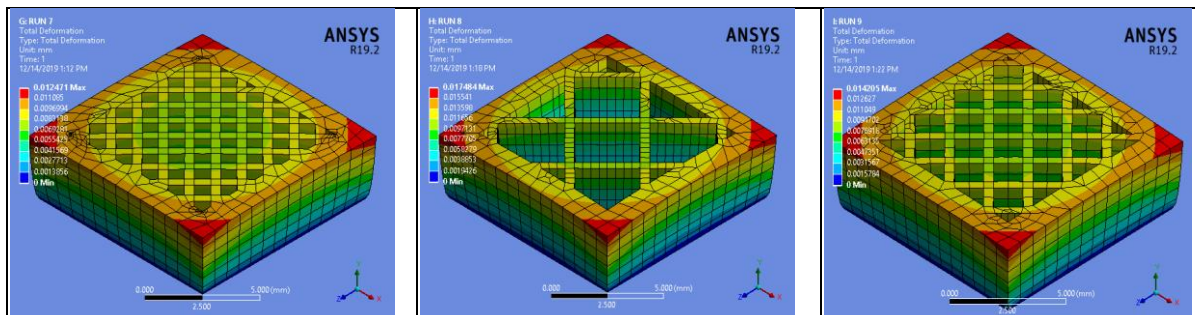


Figure 5: Deformation of the scaffold structure

As the simulation work that had been done on the models, the highest percentage level of porous structure exhibits the highest Equivalent Von-

MisesStrain and Total Deformation. Table 4 below indicates the further detail on Von-Mises Strain and Total Deformation of the samples.

Table 4: Effect of Porosity Level

Run No	Porosity Level (%)	Von-Mises (Max) Strain	Total Deformation, mm
1	64.77	0.011671	0.026989
2	47.46	0.008818	0.018071
3	32.92	0.0059976	0.01432
4	40.23	0.0075263	0.015998
5	27.75	0.0064348	0.013289
6	54.22	0.0090269	0.02115
7	22.62	0.0060161	0.012471
8	44.37	0.0080438	0.017484
9	32.08	0.0067888	0.014205

By referring Figure 6 and 7, the trend of strain and deformation were increasing along with increasing of porosity. Deformations with these loads may have a strong influence on the microstructure of the scaffold, as the design and width of the pores may be changed, resulting in a difference in the permeability of the scaffold.

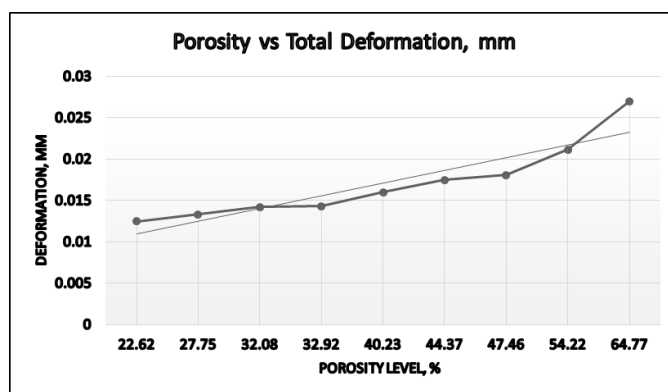
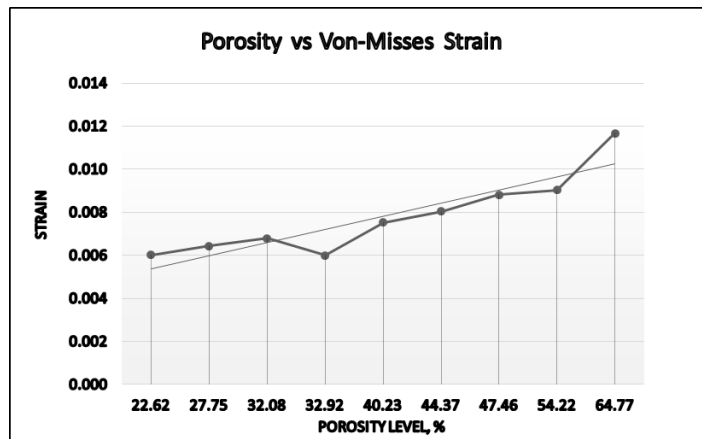


Figure 7: Relationship between Deformation and Porosity Level

Figure 6: Relationship between Strain and Porosity Level

It is possible to observe that higher structure porosity leads to lower structure resistance to deformation. According to Wahid et al., several experiments found 64% porosity and below are appropriate levels to preserve mechanical and fatigue tolerance[13]. Furthermore, this quality depends on several factors, such as material type, mode of processing and

request. As shown by Figure 6 and 7 above, as the porosity level increased, it seems the deformation trend is linearly proportional. Meanwhile, at a porosity of 32.92%, the strain value experiences a slight decrement. However, it is suggested that further research could be carried out by varying the porosity levels in order to have a clear understanding on the deformation.

#### 4. CONCLUSION

In this research, the effect of porosity level on the strain and total deformation was investigated using FEA analysis. As the porosity level increased, the total deformation and equivalent von-mises strain also increased. The impact of printing parameters on the porosity level had been analyzed, therefore, several conclusion can be drawn:

- i. The strain and deformation increased as the porosity level increased. This is due to the bonding strength between the structure itself. Due to high structure porosity, the bonding strength between the infill support and the part shell becomes lower. Thus, these high porosity levels make the structure more ductile permitting larger deformation to occur.
- ii. In scaffold structure, a porosity level of certain value needs to be used to allow the cell growth in bone tissue. Thus, a certain level of deformation needs to be included in designing the scaffold structure.

The limitation of the simulation process provides room for further investigation. The layer height of the printed scaffold is not very significant to be evaluated using simulation as its adhesive and bonding strength between layers might affect its microstructure. Thus, the actual experimental work needs to be executed to overcome this limitation where the full capability of the scaffold can be tested.

#### REFERENCES

1. N. Guo and M. C. Leu, "Additive manufacturing: Technology, applications and research needs," *Front. Mech. Eng.*, vol. 8, no. 3, pp. 215–243, 2013.
2. L. Yuan, S. Ding, and C. Wen, "Additive manufacturing technology for porous metal

implant applications and triple minimal surface structures: A review," *Bioact. Mater.*, vol. 4, no. 1, pp. 56–70, 2019.

3. Z. Chen, "Fabrication and research of 3D complex scaffolds for bone tissue engineering based on extrusion deposition technique Fabrication and Research of 3D Complex Scaffolds for Bone Tissue Engineering Based on Extrusion Deposition Technique By," Thesis, p. 211, 2017.
4. D. Ahn, J. H. Kweon, S. Kwon, J. Song, and S. Lee, "Representation of surface roughness in fused deposition modeling," *J. Mater. Process. Technol.*, vol. 209, no. 15–16, pp. 5593–5600, 2009.
5. M. H. Too et al., "Investigation of 3D non-random porous structures by fused deposition modelling," *Int. J. Adv. Manuf. Technol.*, vol. 19, no. 3, pp. 217–223, 2002.
6. S. Jyoti, S. Bose, H. L. Hosick, and A. Bandyopadhyay, "Development of controlled porosity polymer-ceramic composite scaffolds via fused deposition modeling," vol. 23, pp. 611–620, 2003.
7. A. Owida and R. Chen, "Artery vessel fabrication using the combined fused deposition modeling and electrospinning techniques," vol. 1, no. September 2009, pp. 37–44, 2011.
8. Y. Lai et al., "Osteogenic magnesium incorporated into PLGA/TCP porous scaffold by 3D printing for repairing challenging bone defect," *Biomaterials*, vol. 197, no. September 2018, pp. 207–219, 2019.
9. L. Zhao et al., "Bionic design and 3D printing of porous titanium alloy scaffolds for bone tissue repair," *Compos. Part B Eng.*, vol. 162, no. August 2018, pp. 154–161, 2019.
10. A. H. Aghajanian, B. A. Khazaei, M. Khodaei, and M. Rafienia, "Fabrication of Porous Mg-Zn Scaffold through Modified Replica Method for Bone Tissue Engineering," *J. Bionic Eng.*, vol. 15, no. 5, pp. 907–913, 2018.
11. E. T. W. Tan, J. M. Ling, and S. K. Dinesh, "The feasibility of producing patient-specific acrylic cranioplasty implants with a low-cost 3D printer," *J. Neurosurg.*, vol. 124, no. 5, pp. 1531–1537, 2016.
12. M. Kahl, M. Gertig, P. Hoyer, O. Friedrich, and

- D. F. Gilbert, "Ultra-Low-Cost 3D Bioprinting: Modification and Application of an Off-the-Shelf Desktop 3D-Printer for Biofabrication," *Front. Bioeng. Biotechnol.*, vol. 7, no. July, pp. 1–12, 2019.
13. Z. Wahid, M. K. A. M. Ariffin, B. T. H. T. Baharudin, M. I. S. Ismail, and F. Mustapha, "ABAQUS Simulation of Different Critical Porosities Cubical Scaffold Model," *IOP Conf. Ser. Mater. Sci. Eng.*, vol. 530, p. 012018, 2019.
14. D. Bourell et al., "Fused deposition modeling of patient specific polymethylmethacrylate implants," *Rapid Prototyp. J.*, vol. 16, no. 3, pp. 164–173, 2010.